Data-Driven Performance Evaluation of Geometric Clustering for PolSAR Data Analysis

Gabriel Vasile

DATA-DRIVEN PERFORMANCE EVALUATION OF GEOMETRIC CLUSTERING FOR POLSAR DATA ANALYSIS

Gabriel Vasile

Univ. Grenoble Alpes, CNRS
GIPSA-lab
Grenoble, France

ABSTRACT

We have introduced in [1] a method for unsupervised classification of PolSAR data, on the manifold of Hermitian positive definite matrices obtained from the polar decomposition. In this paper we investigate the polarimetric information preservation of the Hermitian factor using manifold gradient computation. We provide an algorithm to select the optimum number of classes based on the Calinski-Harabasz criterion in the Riemannian geometry context.

***Index Terms*—** clustering, PolSAR, polar decomposition, Hermitian, factor, unitary factor, Riemannian distance

1. INTRODUCTION

In computer science, clustering methods are divided into several groups, as for example: partitional, hierarchical, density, grid or model-based. While such methods are popular for PolSAR unsupervised classification, centroid-based approaches belonging to the partitional category are the most prevalent. The introduction of the Wishart classifier has been a major milestone in PolSAR unsupervised classification [2]. The initialization of the centroids is obtained by the $H-\alpha$ decomposition. This is applied as a prerequisite and an estimate centroid is provided for each class in the $H-\alpha$ plane (which fixes the number of clusters to eight). After each run, the centroids are updated by averaging the redistributed matrices of each class.

With the constant increase in spatial resolution, different non-Gaussian clustering strategies have been adopted for PolSAR data classification. Based on the conventional product model, we can distinguish two main directions in introducing heterogeneity. By adopting either non-Gaussian target vectors (such as K-, Kummer-U, G_0-distributed clutter models) or compound covariance/coherencies (like scale mixtures, G_0- or K-Wishart models) different classification algorithms have been proposed [3, 4].

Being simple and effective, the Wishart classification still remains one of the most employed clustering methods in practical applications. Its popularity and fundamental importance has been proven also by many publications, which by modifying one or more stages in the generic algorithm have arrived to new or improved versions. Notable changes can be found in the: a) initialization and number of clusters [5], b) class assignment logic [6], or c) the distance metric.

The reminder of this paper is organized as follows. Section 2 offers some background on the use Riemannian geometry for unsupervised clustering of PolSAR data. Sections 3 and 4 introduce the manifold sample gradient computation method and the Calinski-Harabasz criterion. Section 5 analyses the experimental results. Finally, the conclusions are discussed in Section 6.

2. RIEMANNIAN GEOMETRY IN POLSAR

It has been more than a decade since the Riemannian manifold embedding is used with PolSAR data, exclusively in evaluating the coherency/covariance matrices. In the general literature, some methods operate directly on the Riemannian manifold, while others operate with projections (i.e., onto the tangent space, embeddings of lower dimension, etc.). The method proposed in [1] fits the first direction. It is described by three different processing stages:

Step 1: The scattering matrix is decomposed using the left[1] polar decomposition, to obtain the Hermitian $\mathbf{H}$ and unitary $\mathbf{U}$ factors:

$$\mathbf{S}=\mathbf{U}\mathbf{H}. \tag{1}$$

Step 2: An identification of coherent scatterers based on the 98^{th} percentile criterion proposed by Lee et al. [7] is performed, at first. For the coherent scatterers, no additional steps are needed and the Hermitian factors are used directly for clustering (Step 3). With all other pixels, barycenters (centers of mass) are otherwise computed. This is the analogous of a N-look geometrical center of mass estimation in the manifold of Hermitian polar factors. The barycenters $\mathbf{H_0}$ are computed through an iterative method applied in square, local,

[1] Since similar results have been obtained when considering alternatively the left or right polar decomposition, we refer hereafter exclusively to the use of the left polar factorization.

sliding neighbourhoods of fixed size:

$$\arg\min_{\mathbf{H_0}} \sum_{i=1}^{m} d_{geod,\mathbb{P}(n)}(\mathbf{H_0}, \mathbf{H_i})^2. \quad (2)$$

Here, the Affine Invariant Riemannian Metric (AIRM) provides a closed-form distance measure

$$d_{geod,\mathbb{P}(n)}(\mathbf{A}, \mathbf{B}) = ||\log(\mathbf{A}^{-1/2}\mathbf{B}\mathbf{A}^{-1/2})||_F, \quad (3)$$

which can be interpreted as a similarity/dissimilarity criterion. The operation of evaluating the Riemannian barycenters in the manifold of Hermitian factors is designated by the acronym *PolBaRi* (*POL*ar decomposition *BA*rycenters estimation on the *RI*emannian manifold).

Step 3: A modified k-means algorithm is applied to the set of points containing barycenters and coherent Hermitian factors. The computation is kept into the native Riemannian manifold of positive-definite matrices using the AIRM metric to evaluate intercluster separation. Here, the class centers are randomly initialized using the k-means++ seeding with the AIRM distance. Progressively, each (barycenter) matrix from the set obtained in Step 2 is allocated to one of the K classes and the cluster centers are updated. The operation is repeated until the interclass transfer is lower than a predefined threshold.

3. MANIFOLD GRADIENT WITH SOBEL KERNEL

For an extended evaluation of the polarimetric information contained in the Hermitian barycenters, a gradient assessment is performed in the manifold space.

The conventional Sobel operator [8], known primarily for edge detection, proposes a sample computation of the first order derivative. It operates with two 3×3 kernel filters. Each of them, used as a sliding window, is convoluted with a spatial neighbourhood of the same size to produce the vertical and horizontal gradient components.

We propose an adaptation for gradient computation on the Hermitian manifold. The same weights as in the Sobel kernels multiply barycenter matrices within a 3×3 spatial neighbourhood, while an adequate metric is used for distance dissimilarity (AIRM with Hermitian matrices). Both the vertical ($\mathbf{G_V}$) and the horizontal ($\mathbf{G_H}$) manifold gradient components are evaluated.

Considering $\mathbf{P}^{\mathrm{i,j}}$ a barycenter matrix located on row i, column j. The following expressions can be written:

$$\mathbf{G_V^{i,j}} = d(\mathbf{P}^{\mathrm{i,j}}_{\uparrow}, \mathbf{P}^{\mathrm{i,j}}_{\downarrow}), \quad (4) \qquad \mathbf{G_H^{i,j}} = d(\mathbf{P}^{\mathrm{i,j}}_{\rightarrow}, \mathbf{P}^{\mathrm{i,j}}_{\leftarrow}), \quad (5)$$

where

$$\mathbf{P}^{\mathrm{i,j}}_{\uparrow} = \mathbf{P}^{\mathrm{i\text{-}1,j\text{-}1}} + 2\mathbf{P}^{\mathrm{i\text{-}1,j}} + \mathbf{P}^{\mathrm{i\text{-}1,j+1}} \quad (6)$$

$$\mathbf{P}^{\mathrm{i,j}}_{\downarrow} = \mathbf{P}^{\mathrm{i+1,j\text{-}1}} + 2\mathbf{P}^{\mathrm{i+1,j}} + \mathbf{P}^{\mathrm{i+1,j+1}} \quad (7)$$

$$\mathbf{P}^{\mathrm{i,j}}_{\leftarrow} = \mathbf{P}^{\mathrm{i\text{-}1,j\text{-}1}} + 2\mathbf{P}^{\mathrm{i,j\text{-}1}} + \mathbf{P}^{\mathrm{i+1,j\text{-}1}} \quad (8)$$

$$\mathbf{P}^{\mathrm{i,j}}_{\rightarrow} = \mathbf{P}^{\mathrm{i\text{-}1,j+1}} + 2\mathbf{P}^{\mathrm{i,j+1}} + \mathbf{P}^{\mathrm{i+1,j+1}}. \quad (9)$$

and the magnitude of the gradient is

$$\mathbf{G} = \sqrt{\mathbf{G_H^2} + \mathbf{G_V^2}}. \quad (10)$$

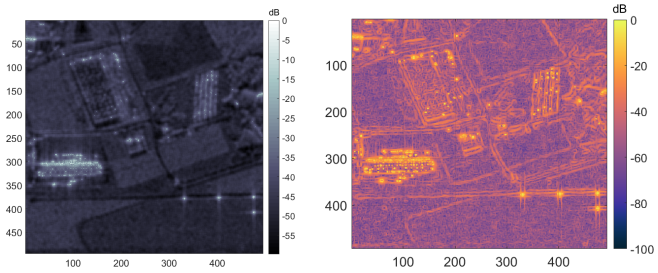

(a) (b)

Fig. 1: Brétigny Dataset, magnitude [dB]: (a) Hermitian barycenters ($\mathbf{h_{11}}$, amplitude, [dB]) and (b) gradient computation for the Hermitian barycenters using the Sobel Filter kernels and the AIRM metric.

Fig. 1 shows the Hermitian barycenters Sobel gradient estimate for the Brétigny PolSAR dataset. The shape of the three important structures from the image (horizontal West-Center of the image, left-oblique North-West and right-oblique North-East) is easily distinguished, as well as the field contours. Bright pixels are clearly isolated.

4. CALINSKI-HARABASZ CRITERION

Given the geometrical nature of the k-means clustering, it is straightforward to define a simple objective criterion for data-driven evaluation of the classification result. By modifying the Calinski-Harabasz (variance ratio) criterion [9] with the AIRM metric, we obtain:

$$\mathrm{CH_k} = \frac{\mathrm{var}_B}{\mathrm{var}_W} \cdot \frac{N-K}{K-1}, \quad (11)$$

$$\mathrm{var}_B = \sum_{i=1}^{K} n_i \cdot d_{geod,\mathbb{P}(n)}(\mathbf{C_i}, \mathbf{H_{tot}})^2, \quad (12)$$

$$\mathrm{var}_W = \sum_{i=1}^{K} \sum_{\mathbf{H_j} \in \mathbf{C_i}} d_{geod,\mathbb{P}(n)}(\mathbf{H_j}, \mathbf{C_i})^2, \quad (13)$$

where N is the total number of pixels in the PolSAR image, K is the number of clusters, $\mathbf{H_{tot}}$ is the overall barycenter of the sample PolSAR data and n_i refers to the number of observations in cluster i, of centroid $\mathbf{C_i}$.

5. RESULTS AND DISCUSSION

Firstly, we aim to assess for any contextual information present with the unitary barycenters. The points for which the barycenters are not convergent are masked-out and can be observed in white in Figs. 2-(a),(b) ($\approx 25\%$ of the image pixels) .

Starting from a complex unitary matrix, $\mathbf{U} \in \mathbb{C}^{2\times 2}$, with

$$\begin{aligned}\mathbf{U} &= \begin{pmatrix} u_{11} & u_{12} \\ u_{21} & u_{22} \end{pmatrix} \\ &= \begin{pmatrix} |u_{11}| \cdot e^{i\varphi_1} & |u_{12}| \cdot e^{i\varphi_2} \\ |u_{21}| \cdot e^{i\varphi_3} & |u_{22}| \cdot e^{i\varphi_4} \end{pmatrix}. \end{aligned} \tag{14}$$

The phase normalized unitary matrix $\mathbf{U_{ph-}}$ can be written in parametric form:

$$\begin{aligned}\mathbf{U_{ph-}} &= \mathbf{U} \begin{pmatrix} e^{-i\varphi_1} & 0 \\ 0 & e^{-i\varphi_4} \end{pmatrix} \\ &= \begin{pmatrix} |u_{11}| & |u_{12}| \cdot e^{i(\varphi_2-\varphi_4)} \\ |u_{21}| \cdot e^{i(\varphi_3-\varphi_1)} & |u_{22}| \end{pmatrix} \qquad (15) \\ &= \begin{pmatrix} \cos\theta & -\sin\theta \cdot e^{-i\phi} \\ \sin\theta \cdot e^{i\phi} & \cos\theta \end{pmatrix} \qquad (16)\end{aligned}$$

After performing the phase normalization, as in (15), the angular θ and phase ϕ parameters are easily obtained for the unitary barycenters of the PolSAR dataset. The results are in Fig. 2-(a) and Fig. 2-(b) respectively, with histograms below the main figures. It is to be mentioned that with the Brétigny dataset about 25% of the image pixels do not attain unitary barycenter convergence.

The θ angle parameter takes values below 25° (Fig. 2-(d)), while the phase absolute values are normally spread in the entire [0°, 180°] interval (Fig. 2-(f)). As example, we can observe the zone corresponding to the building located West-Center, where multiple coherent scatterers are present (red ellipse selection). Here, the θ values approach zero degrees. The phase values present also an extreme (i.e. $\pm$ 180°). Such observations indicate that the phase normalized unitary barycenters at those locations are (almost) identity matrices. In turn, this may also imply that the original unitary polar factors, used in estimating the barycenters, are themselves close to identity. For such a case, the Hermitian polar factors are completely descriptive and (almost) equal to the original scattering matrices. This result confirms the choice from the design of the PolBaRi algorithm [1] of performing the pre-selection of coherent scatterer and attributing to those locations directly the Hermitian factor, without barycenter estimation.

Removing the effect of rotations imposed on the line-of-sight backscattering direction as well as the search of rotation invariant descriptors is of particular interest in polarimetric radar applications. The topic has a significant line of work associated for both coherent and incoherent PolSAR decompositions.

With the polar decomposition, we have shown that the unitary matrices can be described by two random phases and two parametric values (an angle and a phase). With coherent scatterers, discarding the unitary polar factor does not produce significant changes, while for other scatterers the removal of unwanted rotations from the original scattering matrix is highly beneficial. Evidence from both simulated and real data shows that the contextual and spatial information is preserved by the Hermitian polar term. Such observations legitimize the key role of the Hermitian barycenters with the PolBaRi algorithm clustering method.

Finally, in order to find the correct number of classes, different Riemannian k-mean clustering runs are operated on a 300×300 sub-image from the Foulum dataset [1]. Fig. 3 shows the results obtained with $K \in \{4, 7, 16\}$. For each K, $2\times K$ trials have been performed and the maximum $\mathrm{CH_k}$ value has been computed in each case. Fig. 3-(a) illustrates the normalized index $\mathrm{CH_k}$ as function of K. The optimal number of classes with respect to this sub-dataset corresponds to $\arg\max_K(\mathrm{CH_k})$ and equals 7. In Fig. 3-(b), the normalized $\mathrm{CH_k}$ for $K \in \{8, 16\}$ is computed over the full EMISAR Foulum dataset. In this case, the K = 8 provides a much better match.

6. CONCLUSIONS

We have applied the Riemannian metric in the development of a sample gradient algorithm based on the Sobel kernels. It was used for spatial change evaluation with Hermitian and unitary barycenters. In a distinct contribution, we have adapted the Calinski-Harabasz criterion to the Riemannian geometry context.

7. REFERENCES

[1] M. Ciuca, G. Vasile, and M. Congedo, "Geometric clustering of polsar data using the polar decomposition," in *Proceedings. IEEE 2023 International Geoscience and Remote Sensing Symposium*, 2023, pp. 1618–1621.

[2] J.S. Lee, M.R Grunes, T.L. Ainsworth, L.J. Du, D.L. Schuler, and S.R. Cloude, "Unsupervised classification using polarimetric decomposition and the complex Wishart classifier," *IEEE Transactions on Geoscience and Remote Sensing*, vol. 37, no. 5, pp. 2249–2258, 1999.

[3] A.P. Doulgeris, S.N. Anfinsen, and T. Eltoft, "Automated non-Gaussian clustering of polarimetric synthetic aperture radar images," *IEEE Transactions on Geoscience and Remote Sensing*, vol. 49, no. 10, pp. 3665–3676, 2011.

[4] G.C. Hu and Q.H. Zhao, "G0-Wishart distribution based classification from polarimetric SAR images," *ISPRS Annals of the Photogrammetry, Remote Sensing and Spatial Information Sciences*, vol. IV-2/W4, pp. 451–455, 2017.

[5] D. Ratha, A. Bhattacharya, and A.C. Frery, "Unsupervised classification of PolSAR data using a scattering similarity measure

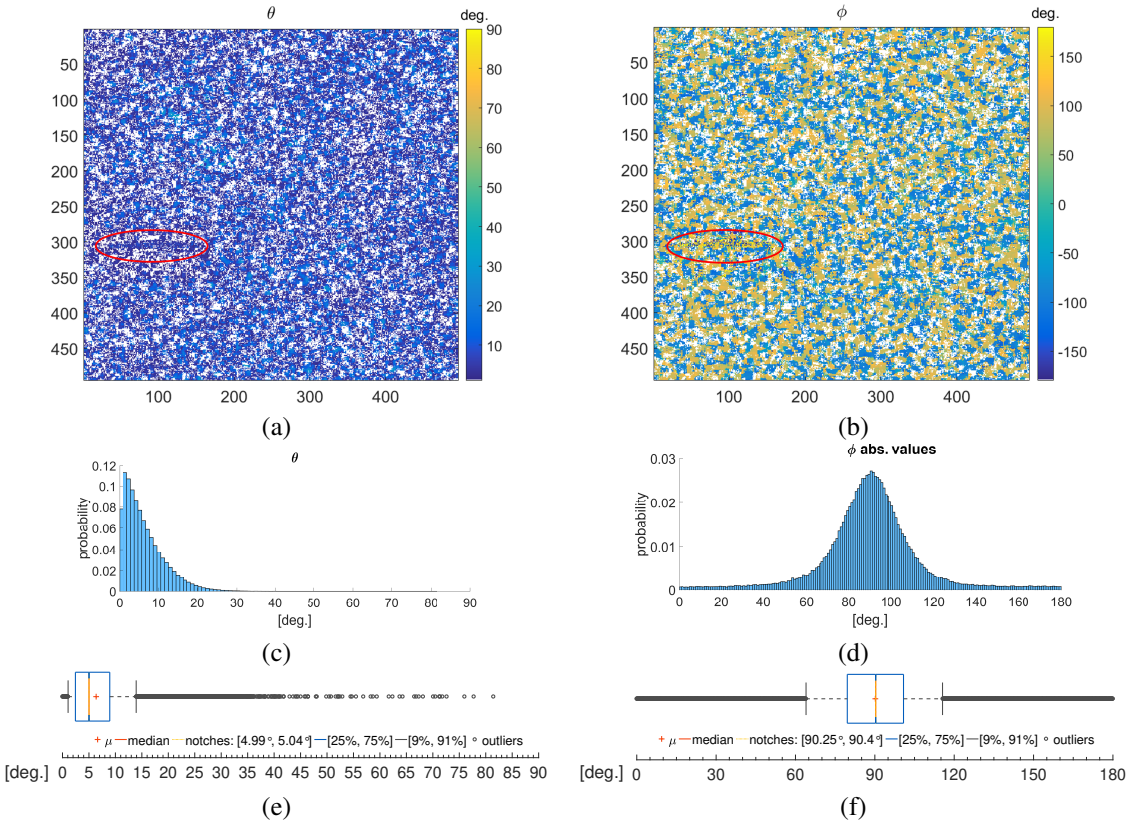

Fig. 2: Brétigny Dataset. (a) Angles obtained from the normalized unitary barycenter matrices [degrees]. (b) Phase values obtained from the normalized unitary barycenter matrices [degrees].
Following statistics are computed excluding white-masked values: (c) Histogram of angles from (a). (d) Histogram of absolute phases from (b). (e) Notches boxplot with mean and median values for angles in (a). (f) Notches boxplot with mean and median values for absolute phase values in (b).

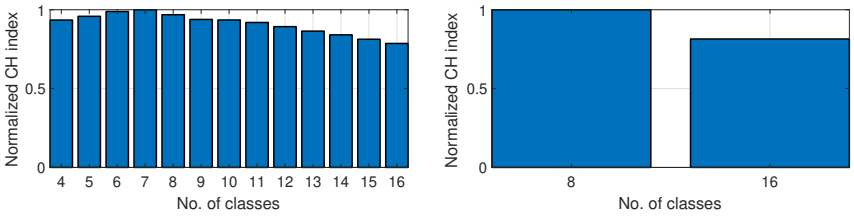

Fig. 3: Foulum Dataset - AIRM Calinski-Harabasz index (normalized display) evaluation. (a) For the data selection in [1]. (b) For the entire Foulum image, if $K = 8$ and $K = 16$.

derived from a geodesic distance," *IEEE Geoscience and Remote Sensing Letters*, vol. 15, no. 1, pp. 151–155, 2018.

[6] J.S. Lee, M.R. Grunes, E. Pottier, and L. Ferro-Famil, "Unsupervised terrain classification preserving polarimetric scattering characteristics," *IEEE Transactions on Geoscience and Remote Sensing*, vol. 42, no. 4, pp. 722–731, 2004.

[7] J. S. Lee, T.L. Ainsworth, Y. Wang, and K.S. Chen, "Polarimetric SAR speckle filtering and the extended Sigma filter," *IEEE Transactions on Geoscience and Remote Sensing*, vol. 53, no. 3, pp. 1150–1160, 2015.

[8] C.C. Lee, "Elimination of redundant operations for a fast Sobel operator," *IEEE Transactions on Systems, Man, and Cybernetics*, vol. SMC-13, no. 2, pp. 242–245, 1983.

[9] T. Caliński and J Harabasz, "A dendrite method for cluster analysis," *Communications in Statistics*, vol. 3, no. 1, pp. 1–27, 1974.